[1.]Mihai ŢĂLU, [2.]Ştefan ŢĂLU

NUMERICAL ANALYSIS OF CYLINDRICAL FUEL TANKS THERMAL BEHAVIOUR

[1.]University of Craiova, Faculty of Mechanics, Department of Applied Mechanics & Civil Engineering, Craiova, ROMANIA
[2.]Technical University of Cluj-Napoca, Research, Development and Innovation Management (DMCDI), Cluj-Napoca, ROMANIA

Abstract: This study describes assumptions, goals, methods, results and a conclusion related to the thermal behavior of three different pressurized cylindrical fuel tanks with the same lateral cover, but with various head covers geometries. A finite element analysis (FEA) is performed across the fuel tank walls to determine the specific key performance indicators and to determine the advantageous fuel tank geometry. The accuracy of the numerical model is shown by the computed results.

Keywords: automotive industry, corrosion, industrial engineering design, optimization methods, pressurized cylindrical fuel tank, temperature resistance, thermal behavior

1. INTRODUCTION

In recent years a large investigation based on innovative concepts has been undertaken on the fuel tanks market with an extensive program of experiments and numerical simulations [1-6], resulting in key information in terms of weight, cost, ergonomics, safety, environmental compatibility and user friendliness [7-13]. Finite element analysis (FEA) and computational fluid dynamics (CFD) are used in computer-aided engineering (CAE) to solve, optimize and validate 3-D geometrical models to ensure that quality, performance, and safety standards are met. On the other hand, these ones can be used in the standard design process and offer a significantly speed/cost advantage compared to experimental tests [14-18]. Based on these numerical simulations, the main areas of interest of the majority of the studies has been the Von Mises stress and linear deformation distribution of the tank walls and the heat transfer across the tank walls [14-18].

In the automotive industry, the fuel tanks are made from aluminum alloys or various types of steel, in a number of different types, weights and sizes for safely storing fuel: compressed natural gas (CNG) or liquefied petroleum gas (LPG) [10-14].

In CAE design and fabrication of fuel tanks with high conformity factors, light weight, and feasible for production level manufacturing: specific structure variables [14, 15], shape design variables [19, 20], design constraints [21], software tools [22-26], and design decision variables [27-29] are used to optimize 3-D geometrical models [30-37]. On the other hand, fuel tanks are subject to the most stringent, destructive, and challenging certification testing requirements set out in regulations and international standards [38].

In the present study, a Finite Element Analysis has been chosen since it is a more suitable tool to investigate the test of temperature resistance at the homologation stage.

2. DESIGN METHODOLOGY

The parameterized modeling of the cylindrical pressurized fuel tank (sectioned to *½*, *¼* or *⅛* of the initial model) was done in the AutoCAD Autodesk 2017 software [39], which was imported to SolidWorks 2017 software [40] for analysis with the: Static, Thermal and Design Study modules. The 3D model tests were thermally loaded at the specified stress state to determine the maximum work temperature T_{max} and the explosion temperature T_r, at the initial and final time of exploitation of the fuel tank.

The design data used in this analysis are:

- the lateral cover with: diameter D = 250 mm and length L = 700 mm;
- the construction material of the sheet metal: steel AISI 4340;
- the maximum static hydraulic pressure: p_{max} = 30 bar;
- the working temperature between the limits: T = -30 ^{0}C to T = 60 ^{0}C;
- the exploitation period of tank: n_a = 20 years;
- the corrosion rate of the material: v_c = 0.1 mm /year.

The temperature resistance means: the maximum temperature at which the resulting stress Von Mises is equal to the admissible stress traction of material $\sigma_{rez} = \sigma_a$ and the explosion temperature is the temperature at which the Von Mises stress attain the breaking stress of the material $\sigma_{rez} = \sigma_r$. Applying the optimization procedure, a laminate sheet of AISI 4340 steel with a thickness of $s = 4^{+0.25}_{-0.6}$ mm is chosen for FEM analyses.

— **The study at temperature resistance of the cylindrical pressurized tank with head covers connected with circular arcs**

The parameterized model of tank (as shown in Figure 1) and the sketch of head cover connected with circular arcs (as shown in Figure 2) are given bellow.

Figure 1. The parametric model of tank with head covers connected with circular arcs

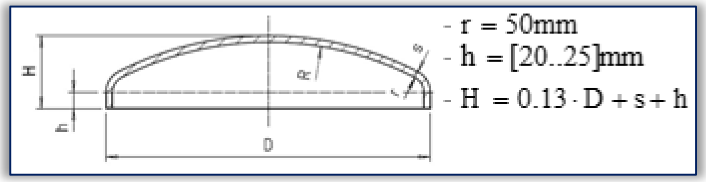

Figure 2. The sketch of head cover connected with circular arcs

After design optimization a laminate sheet of AISI 4340 steel with a thickness of $s = 5.5^{+0.25}_{-0.6}$ mm it was chosen for the manufacturing process (as shown in Figure 3). Next dimensions were obtained for the head cover connected with circular arcs: h = 20 mm, r = 50 mm and H = 75 mm.

The following numerical results were obtained for Von Mises stress distribution at $n_a = 0$ years: $T_{max} = 212.95^0$C, with the corresponding stress distribution (as shown in Figures 3a and 3b). and $T_r = 332.85^0$C, with the corresponding stress distribution (as shown in Figure 3c and 3d).

The graphs of Von Mises stress distribution were shown on the sectioned model at 1/8 in figures 4a and 4c and in figures 4b and 4d for the entire model.

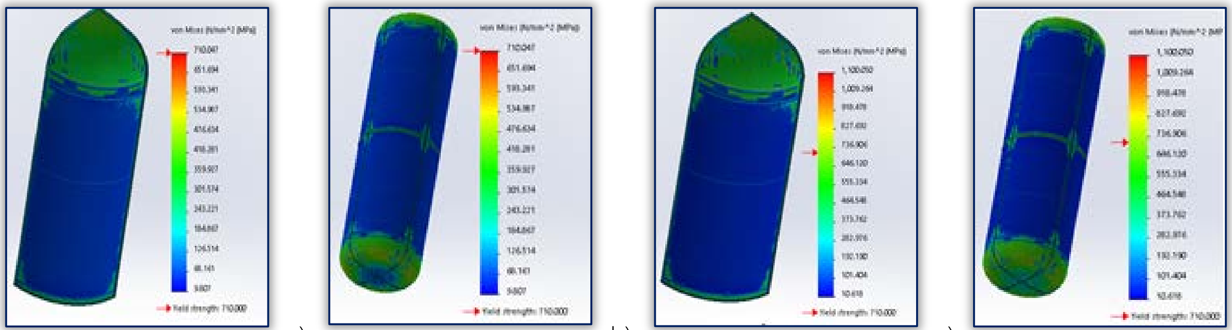

a) b) c) d)

Figure 3. The graphs of Von Mises stress distribution for $n_a = 0$ years: a) and b) at the temperature T_{max}; c) and d) at the explosion temperature T_r

The following numerical results were obtained for Von Mises stress distribution at $n_a = 20$ years: $T_{max} = 135.5^0$C, with the corresponding stress distribution (as shown in Figures 4a and 4b); $T_r = 312.65^0$C, with the corresponding stress distribution (as shown in Figures 4c and 4d).

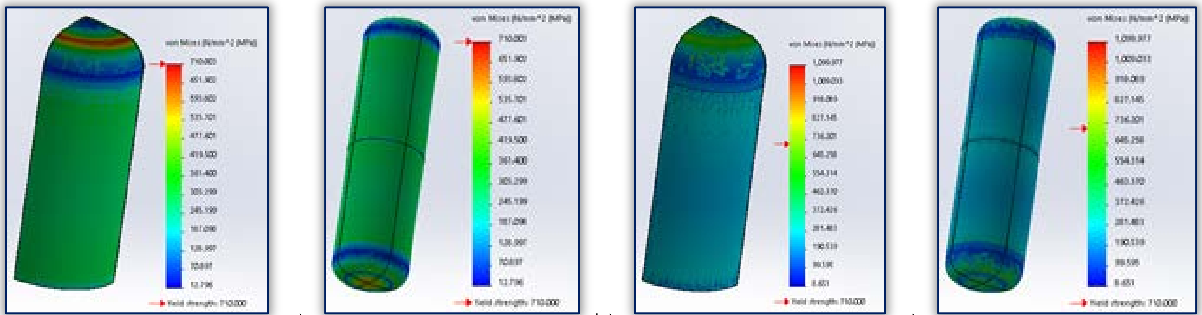

a) b) c) d)

Figure 4. The graphs of Von Mises stress distribution for $n_a = 20$ years: a) and b) at the temperature T_{max}; c) and d) at the explosion temperature T_r

— **The study at temperature resistance of the cylindrical pressurized tank with flat head covers**

The parameterized model of tank (as shown in Figure 5) and the sketch of the flat head cover (as shown in Figure 6) are given bellow.

After design optimization a laminate sheet of AISI 4340 steel with a thickness of $s = 8.5^{+0.25}_{-0.6}$ mm it was chosen for the manufacturing process (as shown in Figure 6). Next dimensions were obtained for the flat head cover: h = 20 mm, r = 50 mm and H = 70 mm.

Figure 5. The parametric model of tank with flat head covers

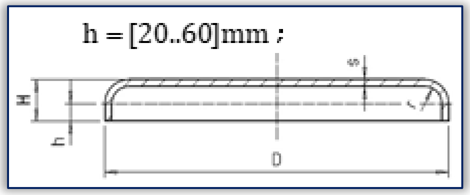

Figure 6. The sketch of flat head cover

The following numerical results were obtained for Von Mises stress distribution at $n_a = 0$ years: $T_{max} = 226.3^0C$, with the corresponding stress distribution (as shown in Figures 7a and 7b); and $T_r = 365.35^0C$, with the corresponding stress distribution (as shown in Figures 7c and 7d).

The graphs of Von Mises stress distribution were shown on the sectioned model at 1/8 in figures 7a and 7c and in figures 7b and 7d for the entire model.

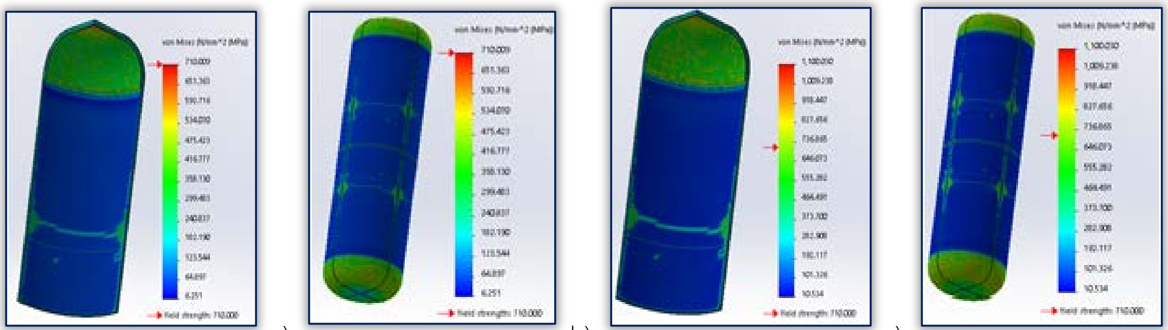

a) b) c) d)

Figure 7. The graphs of Von Mises stress distribution for $n_a = 0$ years: a) and b) at the temperature T_{max}; c) and d) at the explosion temperature T_r

The following numerical results were obtained for Von Mises stress distribution at $n_a = 20$ years: $T_{max} = 163.9^0C$, with the corresponding stress distribution (as shown in Figures 8a and 8b); $T_r = 308.85^0C$, with the corresponding stress distribution (as shown in Figures 8c and 8d).

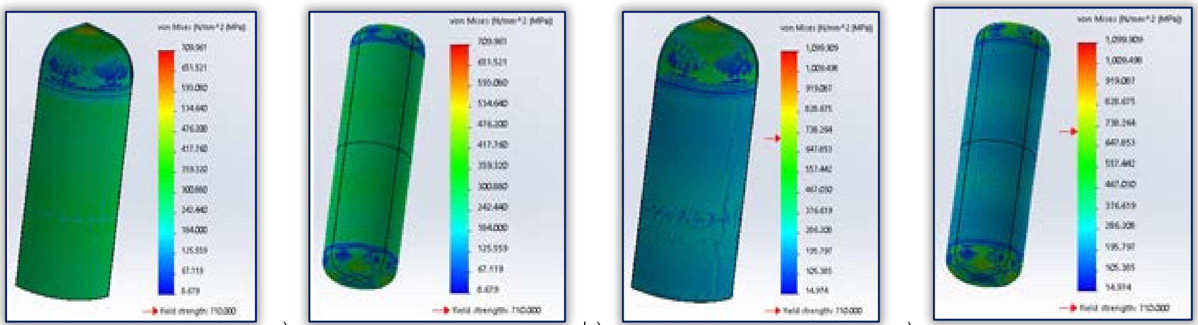

a) b) c) d)

Figure 8. The graphs of Von Mises stress distribution for $n_a = 20$ years: a) and b) at the temperature T_{max}; c) and d) at the explosion temperature T_r

— **The study at temperature resistance of the cylindrical pressurized tank with back head cover connected with circular arcs**

The parameterized model of tank (as shown in Figure 9) and the sketch of the back head cover connected with circular arcs (as shown in Figure 10) are given bellow.

Figure 9. The parametric model of tank with back head covers connected with circular arcs

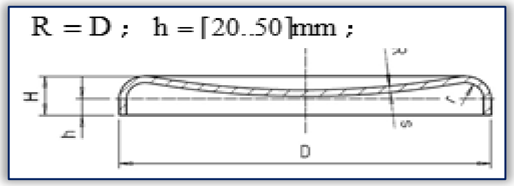

Figure 10. The sketch of back head cover connected with circular arcs

After design optimization a laminate sheet of AISI 4340 steel with a thickness of $s = 8^{+0.25}_{-0.6}$ mm it was chosen for the manufacturing process (as shown in Figure 10). Next dimensions were obtained for the back head cover connected with circular arcs: h = 12 mm, r = 22.5 mm and H = 34.5 mm.

The following numerical results were obtained for Von Mises stress distribution at $n_a = 0$ years: $T_{max} = 209.2^0C$, with the corresponding stress distribution (as shown in Figures 11a and 11b); $T_r = 352.35^0C$, with the corresponding stress distribution (as shown in Figures 11c and 11d).
The graphs of Von Mises stress distribution were shown on the sectioned model at 1/8 in figures 11a and 11c and in figures 11b and 11d for the entire model.

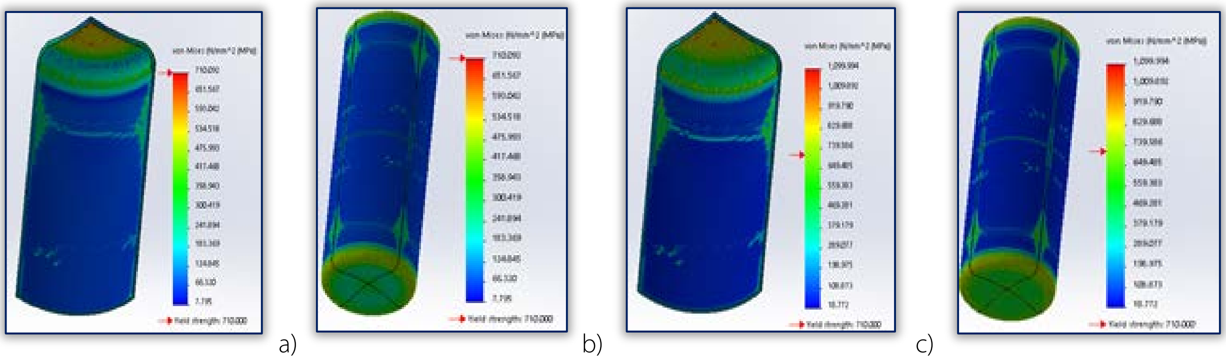

a) b) c) d)

Figure 11. The graphs of Von Mises stress distribution for $n_a = 0$ years: a) and b) at the temperature T_{max}; c) and d) at the explosion temperature T_r

The following numerical results were obtained for Von Mises stress distribution at $n_a = 20$ years: $T_{max} = 154.92^0C$, with the corresponding stress distribution (as shown in Figures 12a and 12b); $T_r = 305^0C$, with the corresponding stress distribution (as shown in Figures 12c and 12d).

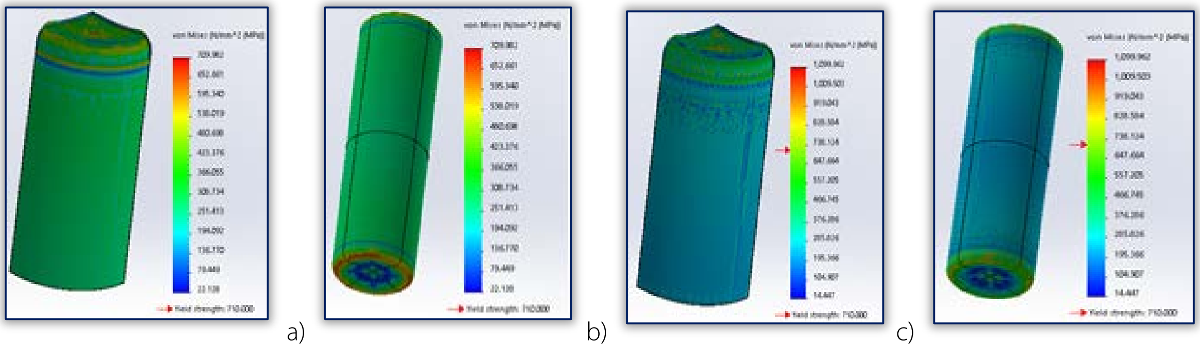

a) b) c) d)

Figure 12. The graphs of Von Mises stress distribution for $n_a = 20$ years: a) and b) at the temperature T_{max}; c) and d) at the explosion temperature T_r

The linear deformation corresponding to the extreme temperatures were also computed.
The numerical values of state of stress and linear resultant deformation of the tanks are given in Table 1.

Table 1. The Von Mises stress and deformation of tanks at temperatures T_{max} and T_r

No.	The type of cylindrical tank	n_a[year]	$T_{max}[^0C]$	u_{max}[mm]	$T_r[^0C]$	u_r[mm]
			$\sigma_a = 710$ MPa		$\sigma_r = 1100$ MPa	
1	Tank with head covers connected with circular arcs	0	212.95	1.001	332.85	1.171
		20	135.50	2.480	312.65	2.785
2	Tank with flat head covers	0	226.30	0.716	365.35	0.922
		20	163.90	1.654	308.85	1.841
3	Tank with back head covers connected with circular arcs	0	209.20	0.957	352.35	1.127
		20	154.92	2.080	305	2.263

The graphical representations of $T_{max}(n_{tank})$ and $T_r(n_{tank})$ depending on the number's tank as specified in Table 1, computed for the initial and the final time of exploitation are shown in Figures 13 and 14.
The graphical representations of $T_{max}(n_{tank})$ and $T_r(n_{tank})$ depending on the number's tank as specified in Table 1, computed for the initial and the final time of exploitation (arranged on the same graph) are shown in Figures 15 and 16.
The graphical representations of $T_{max}(n_a, n_{tank})$ and $T_r(n_a, n_{tank})$ are shown in Figures 17 and 18.
The graphical representations of $u_{max}(n_{tank})$ and $u_r(n_{tank})$ depending on the number's tank as specified in Table 1, computed for the initial and the final time of exploitation are shown in Figures 19 and 20.
The graphical representations of $u_{max}(n_{tank})$ and $u_r(n_{tank})$ depending on the number's tank as specified in Table 1, computed for the initial and the final time of exploitation (and arranged on the same graph for T_{max} and T_r) are shown in Figures 21 and 22.

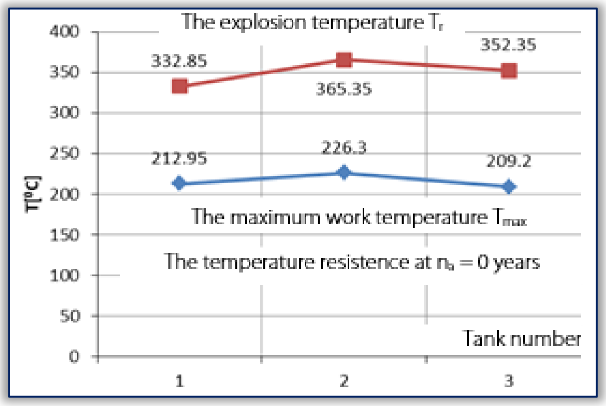

Figure 13. The graphs of $T_r(n_{tank})$ and $T_{max}(n_{tank})$ at $n_a = 0$ years

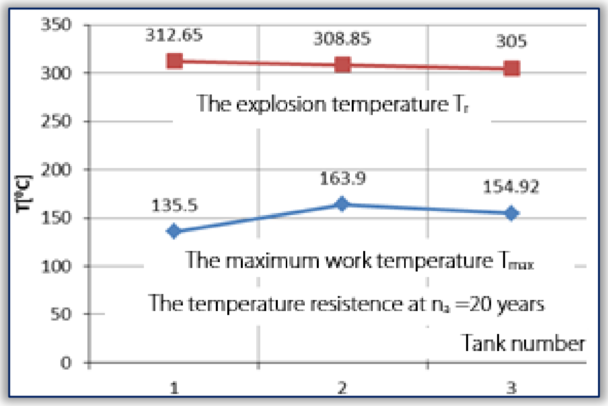

Figure 14. The graphs of $T_r(n_{tank})$ and $T_{max}(n_{tank})$ at $n_a = 20$ years

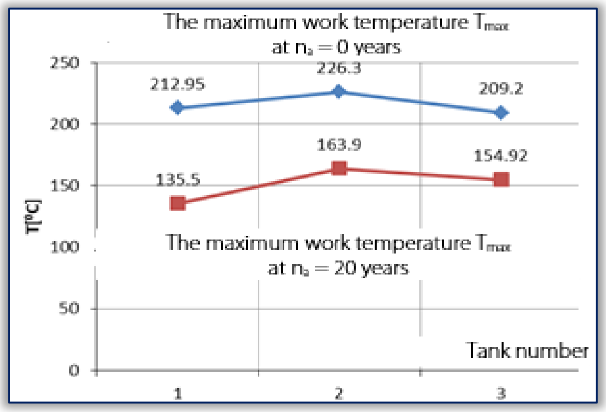

Figure 15. The graphs of $T_{max}(n_{tank})$ at $n_a = 0$ and 20 years

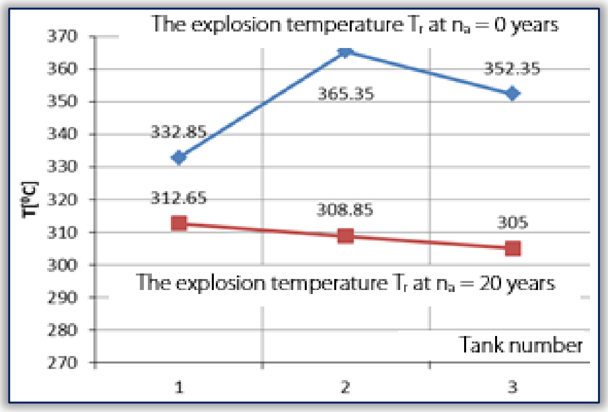

Figure 16. The graphs of $T_r(n_{tank})$ at $n_a = 0$ and 20 years

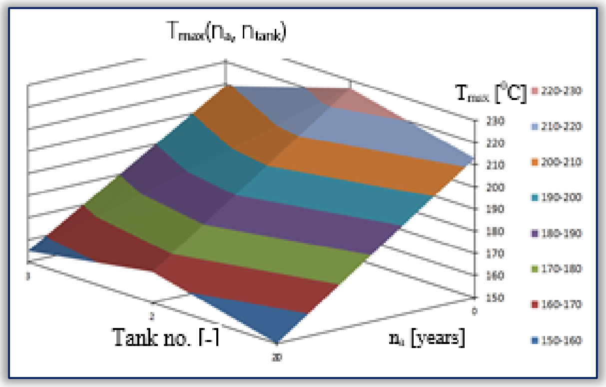

Figure 17. The 3D graph of $T_{max}(n_a, n_{tank})$

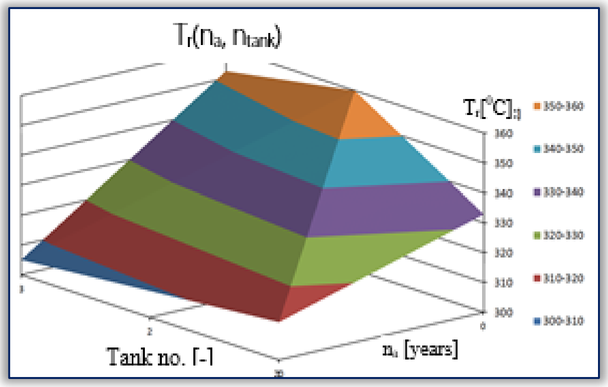

Figure 18. The 3D graph of $T_r(n_a, n_{tank})$

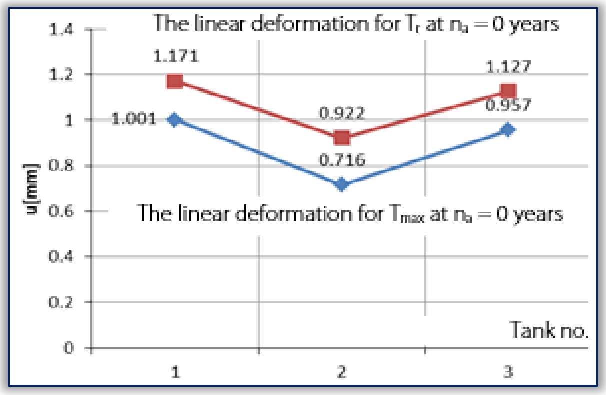

Figure 19. The graphs of $u(n_a)$ for T_r and T_{max} at $n_a = 0$ year

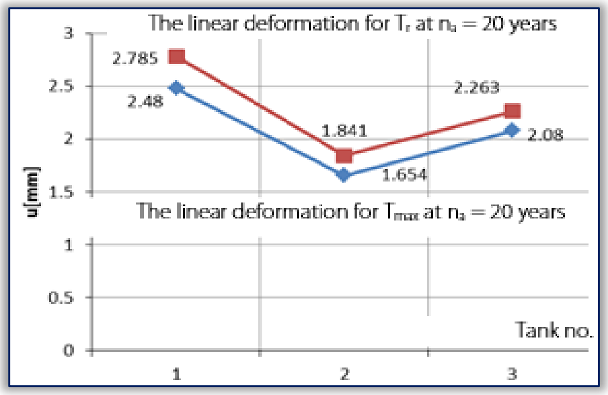

Figure 20. The graphs of $u(n_a)$ for T_r and T_{max} at $n_a = 20$ years

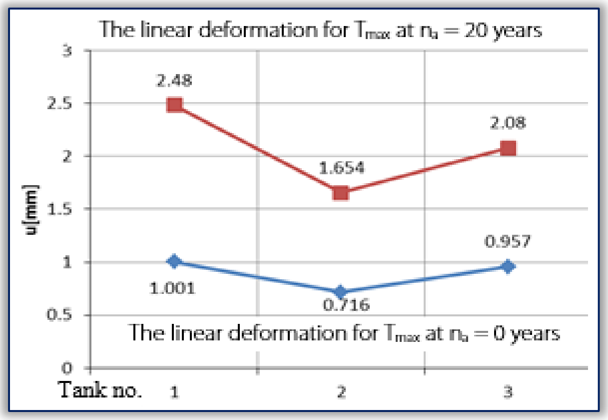

Figure 21. The graphs of $u(n_a, n_{tank})$ for T_{max}

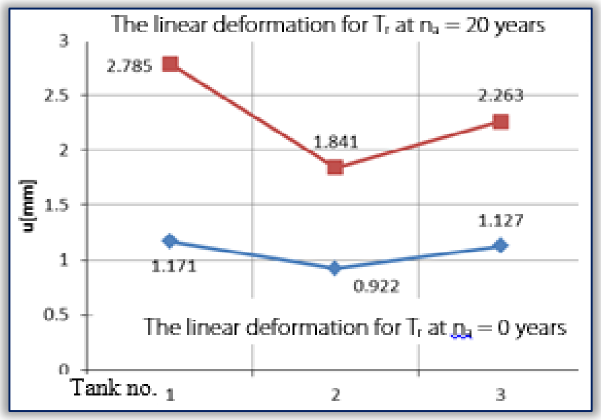

Figure 22. The graphs of $u(n_a, n_{tank})$ for T_r

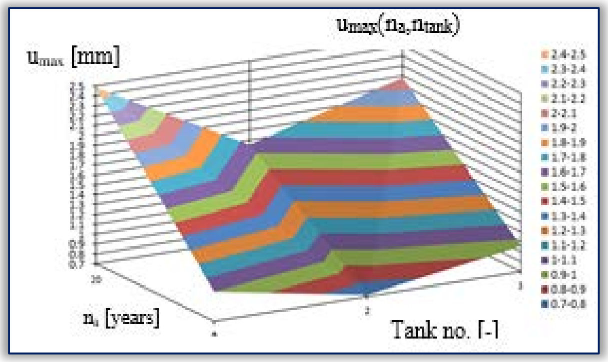

Figure 23. The 3D graph of $u_{max}(n_a, n_{tank})$

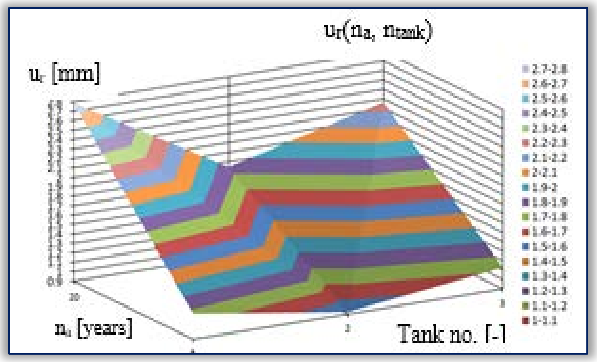

Figure 24. The 3D graph of $u_r(n_a, n_{tank})$

The graphical representations of $u_{max}(n_a, n_{tank})$ and $u_r(n_a, n_{tank})$ are shown in Figures 23 and 24.

3. DISCUSSION

The tank with flat head covers (at $n_a = 0$ years) has the highest work temperature $T_{max} = 226.3^0C$ and the highest explosion temperature $T_r = 365.35^0C$, while the tank with back head covers connected with circular arcs has the lowest work temperature $T_{max} = 209.2^0C$ (as shown in Figure 13).

The tank with flat head covers (at $n_a = 20$ years) has the highest working temperature $T_{max} = 163.9^0C$; while the tank with head covers connected with circular arcs has the lowest work temperature $T_{max} = 135.5^0C$, (as shown in Figure 14).

The tank with head covers connected with circular arcs (at $n_a = 20$ years) has the highest explosion temperature $T_r = 312.65^0C$, while the tank with back head covers connected with circular arcs has the lowest explosion temperature $T_r = 305^0C$, (as shown in Figure 19).

The tank with head covers connected with circular arcs (at $n_a = 0$ years, for T_{max} and T_r) has the maximum linear deformation $u_{max} = 1.001$ mm and $u_r = 1.171$ mm; while the tank with flat head covers has the lowest deformation $u_{max} = 0.716$ mm and $u_r = 0.922$ mm, (as shown in Figure 19).

The tank with head covers connected with circular arcs (at $n_a = 20$ years, for T_{max} and T_r) has the maximum linear deformation $u_{max} = 2.48$ mm and $u_r = 2.785$ mm; while the tank with flat head covers has the lowest deformation $u_{max} = 1.654$ mm and $u_r = 1.841$ mm, (as shown in Figure 20).

4. CONCLUSIONS

In this study, were analysed the performances related to the thermal behaviour of three different pressurized cylindrical fuel tanks with the same same lateral cover, but with various head covers geometries. The FEA results showed that the temperature resistance, the Von Mises stress and deformation are influenced by the tank geometry.

The highest temperature resistance (at $n_a = 0$ years) was found for the tank with flat head covers, while the lowest temperature resistance was found for the tank with back head covers connected with circular arcs.

The highest temperature resistance (at $n_a = 20$ years) was found for the tank with head covers connected with circular arcs, while the lowest temperature resistance was found for the tank with back head covers connected with circular arcs.

The lowest linear deformation was found for the tank with with flat head cover, while the maximum deformation was found for the tank with head covers connected with circular arcs.

Acknowledgements
- Financial disclosure: Neither author has a financial or proprietary interest in any material or method mentioned.
- Competing interests: The authors declare that they have no significant competing financial, professional or personal interests that might have influenced the performance or presentation of the work described in this manuscript.

References

[1] M.C. Ghiţă, A.C. Micu, M. Ţălu, Ş. Ţălu, E. Adam, Computer-Aided Design of a classical cylinder gas tank for the automotive industry, Annals of Faculty of Engineering Hunedoara - International Journal of Engineering, Hunedoara, Tome XI, Fascicule 4, pp. 59-64, 2013.
[2] M.C. Ghiţă, A.C. Micu, M. Ţălu, Ş. Ţălu, 3D modelling of a gas tank with reversed end up covers for automotive industry, Annals of Faculty of Engineering Hunedoara - International Journal of Engineering, Hunedoara, Tome XI, Fascicule 3, 2013, pp. 195-200, 2013.
[3] M.C. Ghiţă, A.C. Micu, M. Ţălu, Ş. Ţălu, Shape optimization of vehicle's methane gas tank, Annals of Faculty of Engineering Hunedoara - International Journal of Engineering, Hunedoara, Tome X, Fascicule 3, pp. 259-266, 2012.
[4] M.C. Ghiţă, A.C. Micu, M. Ţălu, Ş. Ţălu, 3D modelling of a shrink fitted concave ended cylindrical tank for automotive industry. Acta Technica Corviniensis – Bulletin of Engineering, Hunedoara, Romania, Tome VI, Fascicule 4, pp. 87-92, 2013.
[5] M.C. Ghiţă, C.Ş. Ghiţă, Ş. Ţălu, S. Rotaru, Optimal design of cylindrical rings used for the shrinkage of vehicle tanks for compressed natural gas, Annals of Faculty of Engineering Hunedoara - International Journal of Engineering, Hunedoara, Tome XII, Fascicule 3, pp. 243-250, 2014.
[6] M.C. Ghiţă, A.C. Micu, M. Ţălu, Ş. Ţălu, Shape optimization of a thoroidal methane gas tank for automotive industry, Annals of Faculty of Engineering Hunedoara - International Journal of Engineering, Hunedoara, Tome X, Fascicule 3, pp. 295-297, 2012.
[7] Ş. Ţălu, M. Ţălu, The influence of deviation from circularity on the stress of a pressurized fuel cylindrical tank, Magazine of Hydraulics, Pneumatics, Tribology, Ecology, Sensorics, Mechatronics (HIDRAULICA), no. 4, pp. 34-45, 2017.
[8] M. Bică, M. Ţălu, Ş. Ţălu, Optimal shapes of the cylindrical pressurized fuel tanks, Magazine of Hydraulics, Pneumatics, Tribology, Ecology, Sensorics, Mechatronics (HIDRAULICA), no. 4, pp. 6-17, 2017.
[9] M. Ţălu, The influence of the corrosion and temperature on the Von Mises stress in the lateral cover of a pressurized fuel tank, Magazine of Hydraulics, Pneumatics, Tribology, Ecology, Sensorics, Mechatronics (HIDRAULICA), no. 4, pp. 89-97, 2017.
[10] D. Vintilă, M. Ţălu, Ş. Ţălu, The CAD analyses of a torospheric head cover of a pressurized cylindrical fuel tank after the crash test, Magazine of Hydraulics, Pneumatics, Tribology, Ecology, Sensorics, Mechatronics (HIDRAULICA), no. 4, pp. 57-66, 2017.
[11] M. Ţălu, Ş. Ţălu, Analysis of temperature resistance of pressurized cylindrical fuel tanks, Magazine of Hydraulics, Pneumatics, Tribology, Ecology, Sensorics, Mechatronics (HIDRAULICA), no. 1, pp. 6-15, 2018.
[12] M. Ţălu, Ş. Ţălu, Design and optimization of pressurized toroidal LPG fuel tanks with variable section, Magazine of Hydraulics, Pneumatics, Tribology, Ecology, Sensorics, Mechatronics (HIDRAULICA), no. 1, 2018.
[13] Ş. Ţălu, M. Ţălu, Algorithm for optimal design of pressurized toroidal LPG fuel tanks with constant section described by imposed algebraic plane curves, Magazine of Hydraulics, Pneumatics, Tribology, Ecology, Sensorics, Mechatronics (HIDRAULICA), no. 1, 2018.
[14] J. D. Jani, M. K. Gupta, R. R. Trivedi, Shape optimization of externally pressurized thin-walled end dome closures with constant wall thickness of cylinder vessel with help of Bezier curve, IJESIT, Vol. 2, issue 3, pp. 466-475, 2013.
[15] P.M. Patel, R. Jaypalsinh, Design & optimization of LNG-CNG cylinder for optimum weight, IJSRD - International Journal for Scientific Research & Development, vol. 1, issue 2, pp. 282-286, 2013.
[16] G. Remya, Gopi, B.R. Beena, Finite Element Analysis of GFRP LPG cylinder, IJEDR, vol. 3, issue 4, pp. 642-649, 2015.
[17] E. Abbasi, M. Salmani, Investigation and improvement of corrosion resistance in automotive fuel tank, Advanced Materials Research, Vols. 41-42, pp. 491-497, 2008.
[18] T. Izaki, Y. Sueki, T. Mizuguchi, M. Kurosaki, New steel solution for automotive fuel tanks, Rev. Met. Paris, Vol. 102, no. 9, pp. 613-619, 2005.
[19] Ş. Ţălu, M. Ţălu, CAD generating of 3D supershapes in different coordinate systems, Annals of Faculty of Engineering Hunedoara - International Journal of Engineering, Hunedoara, Tome VIII, Fascicule 3, pp. 215-219, 2010.
[20] Ş. Ţălu, M. Ţălu, A CAD study on generating of 2D supershapes in different coordinate systems, Annals of Faculty of Engineering Hunedoara - International Journal of Engineering, Hunedoara, Tome VIII, Fascicule 3, pp. 201-203, 2010.

[21] Ş. Ţălu, Limbajul de programare AutoLISP. Teorie şi aplicaţii, (AutoLISP programming language. Theory and applications), Cluj-Napoca, Risoprint Publishing house, 2001.
[22] Ş. Ţălu, Reprezentări grafice asistate de calculator (Computer assisted graphical representations), Cluj-Napoca, Osama Publishing house, 2001;
[23] Ş. Ţălu, Grafică tehnică asistată de calculator (Computer assisted technical graphics), Cluj-Napoca, Victor Melenti Publishing house, 2001;
[24] Ş. Ţălu, AutoCAD 2005, Cluj-Napoca, Risoprint Publishing house, 2005.
[25] Ş. Ţălu, M. Ţălu, AutoCAD 2006. Proiectare tridimensională (AutoCAD 2006. Three-dimensional designing), Cluj-Napoca, MEGA Publishing house, 2007.
[26] Ş. Ţălu, AutoCAD 2017, Cluj-Napoca, Napoca Star Publishing house, 2017.
[27] M. Ţălu, Calculul pierderilor de presiune distribuite în conducte hidraulice (Calculation of distributed pressure loss in hydraulic pipelines), Craiova, Universitaria Publishing house, 2016.
[28] M. Ţălu, Pierderi de presiune hidraulică în conducte tehnice cu secţiune inelară. Calcul numeric şi analiză C.F.D. (Hydraulic pressure loss in technical piping with annular section. Numerical calculation and C.F.D.), Craiova, Universitaria Publishing house, 2016.
[29] M. Ţălu, Mecanica fluidelor. Curgeri laminare monodimensionale (Fluid mechanics. The monodimensional laminar flow), Craiova, Universitaria Publishing house, 2016.
[30] Ş. Ţălu, Geometrie descriptivă (Descriptive geometry), Cluj-Napoca, Risoprint Publishing house, 2010.
[31] A. Florescu-Gligore, M. Orban Ş. Ţălu, Cotarea în proiectarea constructivă şi tehnologică (Dimensioning in technological and constructive engineering graphics), Cluj-Napoca, Lithography of The Technical University of Cluj-Napoca, 1998.
[32] A. Florescu-Gligore, Ş. Ţălu, D. Noveanu, Reprezentarea şi vizualizarea formelor geometrice în desenul industrial (Representation and visualization of geometric shapes in industrial drawing), Cluj-Napoca, U. T. Pres Publishing house, 2006.
[33] Ş. Ţălu, C. Racocea, Reprezentări axonometrice cu aplicaţii în tehnică (Axonometric representations with applications in technique), Cluj-Napoca, MEGA Publishing house, 2007.
[34] C. Racocea, Ş. Ţălu, Reprezentarea formelor geometrice tehnice în axonometrie (The axonometric representation of technical geometric shapes), Cluj-Napoca, Napoca Star Publishing house, 2011.
[35] Ş. Ţălu, Micro and nanoscale characterization of three dimensional surfaces. Basics and applications, Napoca Star Publishing House, Cluj-Napoca, Romania, 2015.
[36] C. Bîrleanu, Ş. Ţălu, Organe de maşini. Proiectare şi reprezentare grafică asistată de calculator. (Machine elements. Designing and computer assisted graphical representations), Cluj-Napoca, Victor Melenti Publishing house, 2001.
[37] T. Niţulescu, Ş. Ţălu, Aplicaţii ale geometriei descriptive şi graficii asistate de calculator în desenul industrial (Applications of descriptive geometry and computer aided design in engineering graphics), Cluj-Napoca, Risoprint Publishing house, 2001.
[38] *** Certification tests of LPG and CNG (available at site http://vzlutest.cz/en/certification-tests-of-lpg-and-cng-c3.html).
[39] *** Autodesk AutoCAD 2017 software.
[40] *** SolidWorks 2017 software.

ISSN 1584 - 2665 (printed version); ISSN 2601 - 2332 (online); ISSN-L 1584 - 2665